Published in final edited form as:
Semin Radiat Oncol. 2011 April ; 21(2): 101–110. doi:10.1016/j.semradonc.2010.10.001.

Molecular-imaging-based dose painting – a novel paradigm for radiation therapy prescription

Søren M. Bentzen* and
University of Wisconsin – Madison, Departments of Human Oncology, Medical Physics, Biostatistics and Medical Informatics, K4/316 Clinical Science Center, 600 Highland Avenue, Madison WI 53792, USA

Vincent Gregoire
Center for Molecular Imaging and Experimental Radiotherapy & Radiation Oncology Department, Université catholique de Louvain, St-Luc University Hospital, Avenue Hippocrate 10, B-1200 Brussels, Belgium

Abstract

Dose painting is the prescription of a non-uniform radiation dose distribution to the target volume based on functional or molecular images shown to be indicative of the local risk of relapse. Two prototypical strategies for implementing this novel paradigm in radiation oncology are reviewed: sub-volume boosting and dose painting by numbers. Sub-volume boosting involves the selection of a "target within the target", defined by image segmentation on the basis of the quantitative information in the image or morphologically, and this is related to image based target volume selection and delineation. Dose painting by numbers is a voxel-level prescription of dose based on a mathematical transformation of the image intensity of individual pixels. Quantitative use of images to decide both where and how to delivery radiation therapy in an individual case is also called theragnostic imaging. Dose painting targets are imaging surrogates for cellular or microenvironmental phenotypes associated with poor radioresponsiveness. In this review, the focus is on positron emission tomography (PET) tracers: FDG and choline as surrogates for tumor burden, FLT as a surrogate for proliferation (or cellular growth fraction) and hypoxia sensitive tracers including FMISO, EF3, EF5 and Cu-ATSM as surrogates of cellular hypoxia. Research advances supporting the clinico-biological rationale for dose painting are reviewed as are studies of the technical feasibility of optimizing and delivering realistic dose painted radiation therapy plans. Challenges and research priorities in this exciting research field are defined and a possible design for a randomized clinical trial of dose painting is presented.

1. Dose painting and prescription of radiation therapy

Imaging-based dose painting, the prescription and delivery of a non-uniform dose to the clinical target volume (CTV) is a novel paradigm for prescribing radiation therapy[1–3]. The basic idea is to replace, completely or in part, the morphologically or anatomically defined target volume with a map of the spatial distribution of a specific tumor phenotype that is hypothesized or has been shown to be related to local tumor control after radiotherapy. A

*Corresponding author, bentzen@humonc.wisc.edu.

dose prescription function is then used to transform this map into a map of prescribed doses that can be used as input to an inverse planning optimizer. Two prototypical strategies have been considered in the literature: *sub-volume boosting*[1], where an imaging-defined discrete volume is given an additional 'boost' radiation dose (in which case the prescription function takes only two discrete dose values), or *dose painting by numbers*[2], where a dose is prescribed at the voxel level, and it is left for the dose plan optimizer to arrive at a physically deliverable dose distribution that approximates the desired dose distribution. In the latter case, the prescription function maps a range of image intensities onto a range of doses. Hybrids between the two strategies use a series of nested volumes, often about five or so, with a prescribed dose assigned to each of them.

Theragnostic imaging[2] is the application of the quantitative information in biomedical images to produce a prescribed dose map, i.e. not just a map of *where* to treat but ideally also of the local dose fractionation that will optimize tumor control under specified normal-tissue constraints. Dose painting by numbers relies directly on theragnostic imaging whereas sub-volume boosting could include morphologic as well as image intensities in the definition of the boost volume. However, in practice there is a continuum of dose prescription strategies ranging between these two ideal cases. In this review, the emphasis will be on theragnostic imaging but large parts of the discussion will apply to the case of sub-volume boosting as well.

2. The case for non-uniform dose distributions in radiation therapy

Throughout the first half of the history of cancer radiation therapy, the dosimetric challenge was to deliver a sufficiently high dose to the distal aspect of the tumor seen from the direction of the beam. With the advent of megavoltage radiation therapy technology soon after World War II, parallel opposing fields or non-collinear wedged fields allowed delivery of a near-uniform dose to a fairly large target volume. Target volume selection was generally based on structures identifiable on normal x-rays or during fluoroscopy, often bony landmarks or even on the patient's external anatomy. These target regions were typically rationalized as "…having a high risk of microscopic spread of the disease" and in general no attempt was made to directly visualize the tumor mass. What this meant in effect was that margins around the macroscopic tumor volume were liberal, set-up accuracy and motion management were less of a concern but this relative robustness came at a price: it was difficult to push the prescribed dose much above 60 Gy in 2 Gy fractions without excessive toxicity because of the large volume of normal tissue irradiated.

The development of computed tomography provided an unprecedented capability to visualize the gross tumor volume and this gave the opportunity to test the so-called 3D hypothesis, namely that increasing the conformality between the high-dose and the target volume, it would be possible to increase local tumor control without increasing (late) toxicity[4]. This led to a flurry of phase I, II and III radiation dose escalation trials. The broad conclusion of these have been that dose can be pushed higher to some extent but that at least for some late endpoints there has been an associated increase in toxicity as well.

This raises the question whether more advanced dose escalation strategies are more likely to provide a therapeutic gain? One compelling clinico-biological hypothesis is the *dose painting hypothesis*: 1) local recurrences arise from cellular or micro-environmental niches that are (relatively) resistant at the radiation dose level that can safely be routinely delivered using a uniform dose distribution; 2) molecular and functional imaging will allow spatio-temporal mapping of these regions of relative radioresistance; and 3) advances in radiation therapy planning and delivery technologies facilitates delivery of a graded boost to such

regions which in turn should lead to improved local tumor control with acceptable side effects.

Support for the dose painting hypothesis comes in part from mathematical modeling studies. It has been shown that for a fixed integral dose to a tumor with a uniform spatial radiosensitivity distribution, delivering a uniform dose of radiation will maximize the tumor control probability[5–7]. However, for a non-uniform radiosensitivity distribution, a uniform dose distribution is inferior to a distribution that delivers a relatively higher proportion of the integral tumor dose to the more resistant regions of the tumor [8], i.e. by dose painting. Numerous modeling studies, evaluating dose painting strategies under various radiobiological assumptions, have consistently shown large gains in tumor control probability, in the order of 50% or more[3, 8–13]. It should be emphasized that none of these modeling exercises are *assumption free*. Proving a clinical gain from dose painting will ultimately require evidence from clinical trials. However, there is a large body of experimental and clinical data providing indirect support for the dose painting hypothesis and thereby informing the design and encouraging the conduct of dose painting trials. Also, advances in pre-clinical and theoretical research into dose painting provide an increasingly firm base for rational design of clinical trials that are likely to be informative once they are completed.

3. Dose painting targets

Validation of a dose painting target does not necessarily require a mechanistic understanding of the relationship between dose response and expression of the target. It is a sufficient – and from a bioethical standpoint probably also a necessary – condition that an empirical relationship has been demonstrated between target expression and worse local outcome of radiation therapy. The current interest focuses on three evidence based causes of radiation therapy failure in the clinic: tumor burden, tumor cell proliferation and hypoxia (figure 1).

a. Tumor burden, target volume definition and sub-volume boosting

Clinical outcome data shows the importance of volume of cancer as a driver of local outcome after radiation therapy. It was hypothesized already in the 1970's that microscopic disease could be sterilized with a lower dose; the rule of thumb proposed by Fletcher was that roughly 2/3 of the dose needed to control gross disease would suffice[14]. At the other end of the scale, bulky disease might need a radiation boost dose of 10 to 15 Gy in order to produce a reasonable tumor control probability. The volume of cancer hypothesis gave rise to boost field techniques, now an integral part of radiation therapy practice, for instance in post-operative radiotherapy for breast cancer, or elective irradiation of regions with suspected sub-clinical disease to a lower dose level, for example irradiation of the clinically negative neck in patients with squamous cell carcinoma of the head and neck.

Until recently, CT and MRI, were the only imaging modalities used to delineate the tumor burden or Gross Tumor Volume (GTV) for radiotherapy planning purposes. With the rising availability of PET scanners, more and more studies have been conducted to assess the added value of functional imaging in radiotherapy planning. Among the available tracers for clinical use, FDG is by far the most widely used. Its availability, its high signal-to-background ratio (SBR) and the wide clinical experience accumulated over the years make FDG an attractive tracer for clinical research compared to the other available PET tracers. FDG uptake is commonly considered a good surrogate for tumor cell burden, although various parameters influence FDG uptake and retention, such as the rate of glycolysis, tumor perfusion, proliferation, inflammation and hypoxia[15, 16].

Encouraging data support the use of FDG-PET in target definition and dose painting. In HNSCC, methodological studies have demonstrated that the use of pre-radiotherapy FDG-PET led to a better estimate of the true tumor volume, as defined by the pathological specimens, compared with CT and MRI[17, 18]. Interestingly, when validated segmentation tools were used, the mean FDG-PET-based GTV was consistently smaller than the GTV defined from morphological imaging in all investigated tumor locations and at all time points during radiotherapy, see figure 219–[21]. This finding probably reflects the limited soft tissue discrimination of morphological imaging. The reduction of target volumes defined from FDG-PET translated into significant normal tissue sparing with either 3D-CRT or helical IMRT in "proof of concept" HNSCC studies[18, 20]. This effect was even more impressive when FDG-PET was performed weekly during treatment to allow for dose adaptation as shown in figure 3.

FDG-PET has been used as a dose painting target for sub-volume boosting in a phase I study in locally advanced HNSCC[22]. This approach was proven to be feasible and safe. De Neve's group has also demonstrated that FDG avidity could be used as a target for dose painting by numbers, with a clear dosimetric advantage relative to sub-volume boosting due to a better capability to create peak-dose regions inside the planning target volume[23].

Similar encouraging data have also been reported for non-small-cell lung cancer (NSCLC) where studies have found that FDG-PET volumes were smaller in general than CT-defined GTVs, thus reducing the incidental radiation exposure of the healthy lungs and the esophagus sufficiently to allow a radiation dose escalation[24, 25]. FDG-PET scans also help in tumor delineation in the presence of atelectasis or intra-tumor heterogeneity, and has shown a remarkably good correlation with surgical pathology and patient data26–28.

Limited data are available on GTV delineation and dose adaptation with metabolic tracers other than FDG. In the brain, amino-acids such as methionine (MET) and fluoroethyl-L-tyrosine (FET) have been used for GTV delineation in gliomas and for the differentiation between treatment related changes (pseudo-progression or pseudo-regression) and residual/recurrent tumor[29]. Some data support the use of MET and (DOTATOC) as PET tracers for GTV delineation in meningiomas and glomus tumours29. Yet, no data are available on dose adaptation in these tumors. Limited data are available on the use of ^{11}C-choline-PET for volume selection and delineation in adenocarcinoma of the prostate. Because of its low sensitivity, choline-PET has a limited role in routine clinical practice for defining target volumes in patients with intra-prostatic lesions or with metastatic/recurrent disease[30]. Yet, there are promising preliminary data on the use of choline-PET for target selection and as a means of guiding high dose radiation therapy for recurring nodal disease[31].

A modeling study found that using choline-PET to boost the radiation dose within the prostate resulted in only a modest increase in local control[32]. This modest gain stems from the lack of knowledge of the exact PET sensitivity as well as the fractionation sensitivity, quantified by the α/β ratio, of prostate cancer[33].

b. Proliferation

Tumor cell proliferation is a well established cause of local failure after radiation therapy for many tumor types, most convincingly supported by the evidence from randomized controlled trials of a benefit from accelerated radiation therapy in head and neck squamous cell carcinoma[34] and non-small cell lung cancer[35]. It is likely that patient-to-patient variability in accelerated proliferation seen after cytotoxic insults explains at least some of the variability in treatment outcome seen in the clinic [36, 37]. Intensive research and development has gone into developing ^{11}C-labelled thymidine – initially meant for use as an in vivo parallel to the classical tritiated thymidine assay – and several radiolabelled

halogenated pyrimidine deoxynucleosides as PET imaging tracers of DNA synthesis. However, rapid biodegradation of these compounds leads to radiolabelled metabolites in the blood which complicates image analysis and interpretation[38, 39]. Most current interest centers on another radiofluorinated thymidine analog: 3'-Deoxy-3'-[^{18}F]fluorothymidine (FLT). FLT is a terminator of the growing DNA chain and is therefore only incorporated into DNA during synthesis to a very limited extent. However, it is retained in cells after phosphorylation by the thymidine kinase 1 (TK1) enzyme[40]. TK1 is differentially expressed in the late G_1 and S phases but is practically absent in G_0 cells[41]. Thus, although FLT is often referred to as a "proliferation tracer", it actually provides a map of the local *growth fraction* of tumor cells. Consistent with this, the SUV of FLT has been shown in several clinical studies to correlate with the cell-cycle specific Ki-67 index as assessed by immunohistochemistry in biopsies[42–48]. One negative study failed to detect such a correlation in 8 patients with esophageal cancer49. However, in addition to the issue of limited statistical power, the range of Ki-67 indices in the tumors included in this particular study seems atypically narrow and concentrated in the upper end of the range seen in larger series of patients with this disease50. In addition to the data showing that FLT is an imaging surrogate for the tumor cell growth fraction, there are data from animal studies demonstrating sensitivity of FLT PET to detect the growth inhibitory response induced by molecular targeted agents, cytotoxic drugs or ionizing radiation in mouse tumor models (for a recent review see Barwick et al.51), and of androgen ablation in a hormone-sensitive murine prostate tumor model52.

FLT PET scans at baseline and 2 weeks into fractionated radiotherapy have been used to define targets for sub-volume boosting in a recent radiation therapy planning study53. In the absence of direct clinical evidence for an association between these regions and a subsequent local treatment failure, the biological rationale for this boost strategy is still not completely clear. Part of the concern arises from our current understanding of the biology of accelerated proliferation. There is emerging evidence from experimental and clinical studies that accelerated tumor cell repopulation is an actively-controlled biological response to a trauma rather than a simple consequence of high proliferative activity at the onset of therapy. A study by Begg et al.[54] of 476 patients with head and neck squamous cell carcinoma (HNSCC) showed that pre-treatment cell kinetics was *not* predictive of outcome of fractionated radiation therapy. Furthermore, a separate study of the pre-treatment tumor cell growth fraction, assessed by the Ki-67 labeling index from immunohistochemistry (IHC) on biopsies from 402 patients with HNSCC, found this to be *inversely* associated with a benefit from randomized allocation to strongly accelerated radiation therapy[55]. These observations discourage the use of proliferation at baseline as a theragnostic target for dose painting. Redefining the boost volume after two weeks of radiation therapy may help overcome this issue, but it is not clear if this is a valid strategy either.

In contrast to simple cell kinetics at baseline, strong expression of the epidermal growth factor receptor (EGFR) was statistically significantly associated with a favorable outcome after randomization to strongly accelerated RT in 304 patients with HNSCC[56]. This finding is consistent with data from the Danish Head and Neck Cancer study group[57, 58], although these studies did not rely exclusively on randomized treatment allocation. Further evidence for the central role of the EGF signaling pathway in the response of HNSCC to fractionated RT comes from the randomized controlled trial showing a clinical benefit from combining radiation therapy with cetuximab, a monoclonal antibody against the EGF receptor59.

Synthesizing all of the above evidence, two promising avenues for proliferation-targeting dose painting are being pursued. One is to assess the proliferative *response* to therapy rather than proliferation at baseline as a dose painting target. However, serial FLT scans during a course of therapy should be interpreted with some care. This is in part because of the

competition between cell killing and (compensatory) proliferation and in part because FLT uptake requires progression in the cell cycle. Studies have demonstrated that inhibition of cell cycle progression prevents FLT uptake[40] and that FLT uptake in vivo is reduced 24 and 48 hours after single doses of radiation of 8 to 20 Gy60, 61, consistent with the well-established mitotic delay after irradiation. While a shorter delay is to be expected after clinically relevant fraction sizes, the mitotic delay could cause a biased assessment of the tumor cell growth fraction if measured shortly after a dose of radiation. The other avenue is direct PET imaging of a major proliferative response pathway, the obvious prime candidate being the EGFR pathway, at least in case of HNSCC where a substantial body of evidence shows that this is a master switch for accelerated repopulation. EGFR expression can be PET imaged using radiolabelled tyrosine kinase inhibitors or antibodies against the extra-cellular domain of the receptor62. Also of potential interest in a radiation oncology context is the emerging possibility[63] to image constitutively active mutant EGFR using ^{124}I-labelled chimeric antibodies that bind to an EGFR epitope exposed only on mutant, overexpressed or activated forms of the receptor.

c. Hypoxia

Hypoxia plays a double role as a consequence and as a driver of malignant progression[64]. As early as 1936, JC Mottram at Mount Vernon Hospital in Northwood, England demonstrated that tumor hypoxia is associated with a poor response to radiation therapy[65]. Large clinical studies have confirmed that hypoxia, assessed by polarographic micro-electrode measurements of partial oxygen pressure or assessed by immunohistochemistry of hypoxia-related endogenous biomarkers in diagnostic biopsies, is associated with malignant progression and a poor outcome after therapy. The strongest evidence exists for squamous cell carcinoma of the head and neck[66, 67], but there is also evidence for several other tumor sites[68] in particular prostate[69–72] and uterine cervix[73, 74].

A number of PET tracers have been developed as hypoxia surrogates for imaging and several new ones are in various stages of preclinical or clinical development[75, 76]. The two tracers with most extensive clinical experience are [^{18}F]fluoromisonidazole (FMISO) and ^{60}Cu-, ^{61}Cu- or ^{64}Cu-labeled Copper(II) diacetyl-di(N^4-methylthiosemicarbazone) (Cu-ATSM). The overall conclusion from about a dozen correlative clinical studies is that there is a statistically significant association between PET-assessed hypoxia at baseline, i.e. before treatment start, and tumor outcome after radiation therapy[13].

Development of new hypoxia sensitive tracers is partly driven by mechanistic considerations of uptake and retention mechanisms. Like FMISO, several of these tracers are [^{18}F]-labeled nitroimidazoles such as FETNIM ([^{18}F]Fluoroerythronitroimidazole), EF5 (2-(2-nitro-1H-imidazol-1-yl)-N-(2,2,3,3,3-[18F]pentafluoropropyl)acetamide), EF3 (2-(2-Nitroimidazol-1H-yl)-N-(3,3,3-trifluoropropyl)acetamide) and [^{18}F]Fluoroazomycinarabinofuranoside (FAZA). There are potentially interesting differences between these tracers[77], as an example FETNIM and FMISO are more hydrophilic than EF3 or EF5; and there is more non-hypoxia related bioreduction of FMISO compared with EF3. Some studies in rodent tumor models also show differences from one tumor type to another as well as an influence of the interval from administration of the tracer to performing the PET scan. It is not clear to what extent these tracers will have clinically relevant differences in performance when used for PET imaging of human tumors in a population of patients. It is likely that there is no consistently superior hypoxia tracer and it is even possible that some of these tracers could provide complementary information. However, in our view, the potential utility of various tracers for defining dose painting targets can only be established from clinical correlative studies, and it is time to conduct such studies to bring the field forward.

As discussed above, FDG may be a valid dose painting target in itself, but it is not a good imaging surrogate of hypoxia. Clinical studies have found no or very limited correlations between FDG uptake and various PET hypoxia tracers[78] and this is consistent with several small animal tumor studies showing a lack of co-localization between FDG on one hand and Cu-ATSM[79], FAZA[80] or EF3[81] on the other, see figure 4.

One concern in the development of hypoxia directed dose painting is the spatio-temporal stability of the PET hypoxia map. Already the pioneering FMISO PET study by Janet Rasey and colleagues[82, 83] showed PET detected reoxygenation in some but not all tumors investigated. It remains a research question whether the initially hypoxic region should be boosted or whether the plan should be adapted to change in hypoxic regions. Spatial variability has also been demonstrated in a subset of HNSCC tumors in scan-rescan studies conducted before the onset of radiation therapy[84]. However, Lee et al.[85] found that boosting the dose to the hypoxic sub-volume on one scan would still lead to a substantial additional dose to the sub-volume that was found to be hypoxic on the repeat scan.

The magnitude of the required dose to control disease in PET hypoxic regions is not clear. Simplistic back-of-an-envelope estimates based on in vitro oxygen enhancement ratios (OER) are likely to be gross overestimates of the dose required in human tumors. Interestingly in this context, Lee et al.[86] found excellent loco-regional tumor control in a series of 20 patients after standard chemoradiation therapy despite the presence of PET detected hypoxia in the primary tumor or in positive nodes at baseline or during fractionated therapy in 18 of these cases.

d. Adaptive dose painting

Adaptive dose painting aims to use imaging as a biomarker of (local) response, typically derived from repeat imaging during radiotherapy compared with a scan at baseline, i.e. before treatment commences. This response map is then used as the input map to adapt the delineated target volume or, in case of dose painting by numbers, the dose distribution so that relatively more dose is applied in regions showing poor response.

A few studies have been conducted so far on FDG-PET-based adaptive treatment in NSCLC. A pilot study of 14 cases reported that an FDG PET scan performed at mid-treatment showed a 44% reduction in GTV in 6 compared with a reduction of 26% on CT[87]. An FDG-PET-based boost dose of 30–102 Gy (mean 58 Gy), or alternatively, a reduction in normal tissue complication probability (NTCP) of 0.4–3% (mean 2%), was deemed clinically feasible in 5 of these 6 patients. However, in a similarly designed study, Gillham et al.[88] concluded that despite tumor shrinkage determined by FDG-PET/CT during treatment, the adaptive-targeting strategy tested in their study would only allow a modest dose escalation.

Response-adaptive dose painting immediately raises the question: When to image? With FDG in HNSCC the signal is weak after 30–40 Gy of chemo-radiation and is not visible after 50 Gy. Similar observations have been made for other tracers. It is likely that useful differentiation according to patient-to-patient variability in response to therapy will have to be assessed after one to three weeks of treatment.

Even after one week of therapy, the PET signal would conceivably mainly reflect doomed cells! No imaging modality can currently distinguish between viable cells that are doomed or not. However, as mentioned above, validation of a dose painting target will come from empirical, clinical evidence rather than from mechanistic considerations also in the case of adaptive dose painting strategies.

4. Dose prescription for dose painting by numbers

The simplest, reasonable, voxel-based prescription function is a linear interpolation between a minimum dose, D_{min}, and a maximum dose D_{max}, as the voxel image intensity, I, varies between its lower and upper bound, I_{min} and I_{max} within the target volume[9, 89]:

$$D(I)=D_{min}+\frac{I-I_{min}}{I_{max}-I_{min}}\cdot(D_{max}-D_{min})$$

A slightly different formulation was proposed by Flynn et al.[90] who proposed a strategy where a voxel-based boost dose was applied to an anatomically defined target sub-volume. The boost was added on top of a uniform dose to the clinical target volume, D_{CTV} such that the mean boost dose was kept equal to a pre-set uniform boost dose, D_{boost}. Using the same notation as above:

$$D(I)=D_{CTV}+\frac{I}{I_{mean}}\cdot D_{boost}$$

This principle for dose prescription is known as dose redistribution[10]. Flynn's formulation still assumes proportionality between image intensity and (boost) dose, but the advantage is that keeping D_{boost} constant produces a 'natural' control dose plan for a hypothetical trial, delivering a uniform boost of the same size but without image guided dose painting. Also Alber and colleagues considered a linear transformation of the image intensity into a prescribed dose but with slightly different constraints on the prescribed dose[91].

The optimal mathematical form of the prescription function is unknown[92] and will depend on the specific tracer. Ideally it should be estimated empirically from radiation dose-response data as a function of tracer uptake level. Several authors have tried to incorporate mechanistic elements in the prescription function, for example Thorwarth et al.[93] who modified the radiosensitivity parameter in a linear-quadratic dose-survival curve according to the retention of FMISO; or Søvik et al.[10] who also used an underlying linear quadratic model of cell survival with direct scaling of the a and b parameters using an analytical, approximate, description of the OER.

While these semi-mechanistic prescription functions may represent useful starting points for empirical estimation of the optimal prescription function, they are obviously over-simplifications of the more complex multi-factorial biology underlying local radioresponsiveness at the voxel level.

5. Delivery of dose painted radiation therapy

Numerous planning studies have shown that sub-volume boosting or multi-level dose painting plans can be optimized using commercial software[65] and that dose-painting-by-numbers plans can be optimized using research software[90, 91, 94]. The technical feasibility of optimizing linac based IMRT plans[9, 65, 93, 95, 96], helical[90, 97] and arc photon[98] IMRT plans as well as intensity modulated proton therapy (IMPT) plans[90, 97] has been documented. Several of these studies have compared the relative merits of various delivery platforms, and – expectedly – delivery technologies with a high number of degrees of freedom and with intrinsically high spatial resolution do better. Overall, it seems fair to say that success in meeting a given set of dose painting plan objectives is less technology dependent than one would have suspected. IMPT plans may show an advantage for certain

configurations of target volumes and critical normal structures, again as one would intuitively expect.

Relatively few feasibility studies have taken the crucial step from planning to delivery of realistic dose painting. However, phantom studies by Kissick et al.[99] have produced encouraging results. Kissick used film dosimetry on a 4D-motion anthropomorphic lung phantom to test the feasibility of helical tomotherapy delivery of a clinically realistic dose painting plan. The authors concluded that delivery was feasible with a relatively modest degradation of the gamma map compared to delivery of the same plan to a static phantom.

6. Research priorities: towards clinical implementation

Molecular-imaging guided dose painting is a compelling concept. Based on current research, modulation of the radiation dose distribution according to local phenotypic or microenvironmental variations in an individual tumor is likely to be technically feasible at a level of spatial resolution comparable to the voxel size in clinical PET images. In view of the complexity of dose painting strategies clinical correlative studies and early clinical trials should be initiated and conducted in parallel with continued pre-clinical research.

What would clinical trials of dose painting look like? Probably not very different from other comparative effectiveness trials! Phase I/II studies of dose painting by FDG defined sub-volume boosting have already been published for patients with HNSCC[22] and further early trials are in progress in this disease and in NSCLC. Pre-operative radiation therapy for rectal adenocarcinoma is another interesting indication where pathological response could be used as an early surrogate endpoint for tumor effect. Also recurrent rectal carcinomas, among many other tumor sites and histologies, have been considered in this context[100]. The obvious attraction of FDG-based dose painting is the wide availability and the extensive clinical experience with this tracer.

The boost dose escalation trial from De Neve's group[22], enrolled 41 patients with HNSCC between 2003 and 2005, 23 at dose level I (total physical dose of 72.5 Gy in 32 fractions to the FDG-PET positive volume), and 18 at dose level II (77.5 Gy in 32 fractions to the PET positive volume). With a median follow-up for surviving patients of 14 months, two cases of dose-limiting Grade 4 toxicity occurred at dose level I. A treatment-related death at dose level II led to termination of the trial. Actuarial 1-year local control was 85% and 87% at the two dose levels. However, 4 of the 9 recurrences seen at the time of analysis occurred in the FDG-defined boost region, raising the possibility that dose should be escalated further if possible without exceeding the acceptable toxicity.

Once the feasibility and safety of the dose painting strategy is established, a phase III trial should be launched with time to loco-regional progression and late toxicity as joint primary endpoints (Figure 5). Recording the pattern of failure and its relation to the PET distribution will be important. Again HNSCC would be an attractive tumor site due to the importance of local control for long-term disease control. To avoid under-treating patients in any of the trial arms, a conservative approach would be to do a dose-painted boost dose only on top of a standard curative dose to the clinical target volume. A PET/CT scan should be performed in all cases with the investigational PET tracer and dose painting by numbers or to a PET defined sub-volume should be planned. To compare like with like, in each patient, the PET defined dose painting plan should be matched with a geometrically defined boost plan delivering the same integral dose to the target volume. The actual plan to be used will be decided by randomization. Although modeling has suggested large gains in tumor control from dose painting, the trial should have a sample size allowing detection of a 15 percentage point improvement in loco-regional control with 90% power. The trial sample size would be about 450 patients, but an adaptive design could be considered. Clearly, this would need a

multi-center or cooperative group format to finish accrual within a reasonable time. Strong data from the early clinical trials will be required to motivate a phase III trial with this sample size and complexity of the intervention. We anticipate that such a trial will be initiated within the next five years.

Reference List

1. Ling CC, Humm J, Larson S, et al. Towards multidimensional radiotherapy (MD-CRT): biological imaging and biological conformality. Int J Radiat Oncol Biol Phys 2000;47(3):551–560. [PubMed: 10837935]
2. Bentzen SM. Theragnostic imaging for radiation oncology: dose-painting by numbers. Lancet Oncol 2005;6(2):112–117. [PubMed: 15683820]
3. Brahme A. Biologically optimized 3-dimensional in vivo predictive assay-based radiation therapy using positron emission tomography-computerized tomography imaging. Acta Oncol 2003;42(2): 123–136. [PubMed: 12801131]
4. Lichter AS. Three-dimensional conformal radiation therapy: a testable hypothesis. Int J Radiat Oncol Biol Phys 1991;21:853–855. [PubMed: 1869476]
5. Webb S, Evans PM, Swindell W, Deasy JO. A proof that uniform dose gives the greatest TCP for fixed integral dose in the planning target volume. Phys Med Biol 1994;39(11):2091–2098. [PubMed: 15560013]
6. Webb S, Nahum AE. A model for calculating tumour control probability in radiotherapy including the effects of inhomogeneous distributions of dose and clonogenic cell density. Phys Med Biol 1993;38(6):653–666. [PubMed: 8346278]
7. Levin-Plotnik D, Hamilton RJ. Optimization of tumour control probability for heterogeneous tumours in fractionated radiotherapy treatment protocols. Phys Med Biol 2004;49(3):407–424. [PubMed: 15012010]
8. Brahme A, Agren AK. Optimal dose distribution for eradication of heterogeneous tumours. Acta Oncol 1987;26(5):377–385. [PubMed: 3426851]
9. Vanderstraeten B, Duthoy W, Gersem WD, Neve WD, Thierens H. [(18)F]fluoro-deoxy-glucose positron emission tomography ([(18)F]FDG-PET) voxel intensity-based intensity-modulated radiation therapy (IMRT) for head and neck cancer. Radiother Oncol 2006;79(3):249–258. [PubMed: 16564588]
10. Sovik A, Malinen E, Bruland OS, Bentzen SM, Olsen DR. Optimization of tumour control probability in hypoxic tumours by radiation dose redistribution: a modelling study. Phys Med Biol 2007;52(2):499–513. [PubMed: 17202629]
11. Stavreva NA, Stavrev PV, Round WH. A mathematical approach to optimizing the radiation dose distribution in heterogeneous tumours. Acta Oncol 1996;35(6):727–732. [PubMed: 8938221]
12. Popple RA, Ove R, Shen S. Tumor control probability for selective boosting of hypoxic subvolumes, including the effect of reoxygenation. Int J Radiat Oncol Biol Phys 2002;54(3):921–927. [PubMed: 12377346]
13. Bentzen SM. Dose painting and theragnostic imaging: towards the prescription, planning and delivery of biologically targeted dose distributions in external beam radiation oncology. Cancer Treat Res 2008;139:41–62. 41–62. [PubMed: 18236711]
14. Fletcher GH. Subclinical Disease. Cancer 1984;53:1274–1284. [PubMed: 6692318]
15. Bos R, Der Hoeven JJ, van Der WE, et al. Biologic correlates of (18)fluorodeoxyglucose uptake in human breast cancer measured by positron emission tomography. J Clin Oncol 2002;20(2):379–387. [PubMed: 11786564]
16. Zhao S, Kuge Y, Mochizuki T, et al. Biologic correlates of intratumoral heterogeneity in 18F-FDG distribution with regional expression of glucose transporters and hexokinase-II in experimental tumor. J Nucl Med 2005;46(4):675–682. [PubMed: 15809491]
17. Daisne JF, Duprez T, Weynand B, et al. Tumor volume in pharyngolaryngeal squamous cell carcinoma: comparison at CT, MR imaging, and FDG PET and validation with surgical specimen. Radiology 2004;233(1):93–100. [PubMed: 15317953]

18. Geets X, Lee JA, Bol A, Lonneux M, Gregoire V. A gradient-based method for segmenting FDG-PET images: methodology and validation. Eur J Nucl Med Mol Imaging 2007;34(9):1427–1438. [PubMed: 17431616]
19. Geets X, Tomsej M, Lee JA, et al. Adaptive biological image-guided IMRT with anatomic and functional imaging in pharyngo-laryngeal tumors: impact on target volume delineation and dose distribution using helical tomotherapy. Radiother Oncol 2007;85(1):105–115. [PubMed: 17562346]
20. Geets X, Daisne JF, Tomsej M, Duprez T, Lonneux M, Gregoire V. Impact of the type of imaging modality on target volumes delineation and dose distribution in pharyngo-laryngeal squamous cell carcinoma: comparison between pre- and per-treatment studies. Radiother Oncol 2006;78(3):291–297. [PubMed: 16499982]
21. Dirix P, Vandecaveye V, De KF, Stroobants S, Hermans R, Nuyts S. Dose painting in radiotherapy for head and neck squamous cell carcinoma: value of repeated functional imaging with (18)F-FDG PET, (18)F-fluoromisonidazole PET, diffusion-weighted MRI, and dynamic contrast-enhanced MRI. J Nucl Med 2009;50(7):1020–1027. [PubMed: 19525447]
22. Madani I, Duthoy W, Derie C, et al. Positron emission tomography-guided, focal-dose escalation using intensity-modulated radiotherapy for head and neck cancer. Int J Radiat Oncol Biol Phys 2007;68(1):126–135. [PubMed: 17448871]
23. Vanderstraeten B, Duthoy W, De GW, De NW, Thierens H. [18F]fluoro-deoxy-glucose positron emission tomography ([18F]FDG-PET) voxel intensity-based intensity-modulated radiation therapy (IMRT) for head and neck cancer. Radiother Oncol 2006;79(3):249–258. [PubMed: 16564588]
24. De Ruysscher D, Wanders S, Minken A, et al. Effects of radiotherapy planning with a dedicated combined PET-CT-simulator of patients with non-small cell lung cancer on dose limiting normal tissues and radiation dose-escalation: a planning study. Radiother Oncol 2005;77(1):5–10. [PubMed: 16019093]
25. van der Wel A, Nijsten S, Hochstenbag M, et al. Increased therapeutic ratio by 18FDG-PET CT planning in patients with clinical CT stage N2-N3M0 non-small-cell lung cancer: a modeling study. Int J Radiat Oncol Biol Phys 2005;61(3):649–655. [PubMed: 15708242]
26. Nestle U, Kremp S, Schaefer-Schuler A, et al. Comparison of different methods for delineation of 18F-FDG PET-positive tissue for target volume definition in radiotherapy of patients with non-Small cell lung cancer. J Nucl Med 2005;46(8):1342–1348. [PubMed: 16085592]
27. Stroom J, Blaauwgeers H, van BA, et al. Feasibility of pathology-correlated lung imaging for accurate target definition of lung tumors. Int J Radiat Oncol Biol Phys 2007;69(1):267–275. [PubMed: 17707281]
28. van Baardwijk A, Bosmans G, Boersma L, et al. PET-CT-based auto-contouring in non-small-cell lung cancer correlates with pathology and reduces interobserver variability in the delineation of the primary tumor and involved nodal volumes. Int J Radiat Oncol Biol Phys 2007;68(3):771–778. [PubMed: 17398018]
29. Grosu AL, Weber WA. PET for radiation treatment planning of brain tumours. Radiother Oncol 2010;96(3):325–327. [PubMed: 20728952]
30. Picchio M, Giovannini E, Crivellaro C, Gianolli L, di MN, Messa C. Clinical evidence on PET/CT for radiation therapy planning in prostate cancer. Radiother Oncol 2010;96(3):347–350. [PubMed: 20708811]
31. Rinnab L, Simon J, Hautmann RE, et al. [(11)C]choline PET/CT in prostate cancer patients with biochemical recurrence after radical prostatectomy. World J Urol 2009;27(5):619–625. [PubMed: 19234708]
32. Niyazi M, Bartenstein P, Belka C, Ganswindt U. Choline PET based dose-painting in prostate cancer--modelling of dose effects. Radiat Oncol 2010;5:23. 23. [PubMed: 20298546]
33. Bentzen SM, Ritter MA. The alpha/beta ratio for prostate cancer: What is it, really? Radiother Oncol 2005;76:1–3. [PubMed: 15990189]
34. Bourhis J, Overgaard J, Audry H, et al. Hyperfractionated or accelerated radiotherapy in head and neck cancer: a meta-analysis. Lancet 2006;368(9538):843–854. [PubMed: 16950362]

35. Saunders M, Dische S, Barrett A, Harvey A, Gibson D, Parmar M. Continuous hyperfractionated accelerated radiotherapy (CHART) versus conventional radiotherapy in non-small-cell lung cancer: a randomised multicentre trial. CHART Steering Committee. Lancet 1997;350(9072):161–165. [PubMed: 9250182]
36. Kim JJ, Tannock IF. Repopulation of cancer cells during therapy: an important cause of treatment failure. Nat Rev Cancer 2005;5(7):516–525. [PubMed: 15965493]
37. Bentzen SM. Repopulation in radiation oncology: perspectives of clinical research. Int J Radiat Biol 2003;79(7):581–585. [PubMed: 14530167]
38. Gardelle O, Roelcke U, Vontobel P, et al. [76Br]Bromodeoxyuridine PET in tumor-bearing animals. Nucl Med Biol 2001;28(1):51–57. [PubMed: 11182564]
39. Christman D, Crawford EJ, Friedkin M, Wolf AP. Detection of DNA synthesis in intact organisms with positron-emitting (methyl- 11 C)thymidine. Proc Natl Acad Sci U S A 1972;69(4):988–992. [PubMed: 4554538]
40. Rasey JS, Grierson JR, Wiens LW, Kolb PD, Schwartz JL. Validation of FLT uptake as a measure of thymidine kinase-1 activity in A549 carcinoma cells. J Nucl Med 2002;43(9):1210–1217. [PubMed: 12215561]
41. Munch-Petersen B, Cloos L, Jensen HK, Tyrsted G. Human thymidine kinase 1. Regulation in normal and malignant cells. Adv Enzyme Regul 1995;35:69–89. 69–89. [PubMed: 7572355]
42. Yap CS, Czernin J, Fishbein MC, et al. Evaluation of thoracic tumors with 18F-fluorothymidine and 18F-fluorodeoxyglucose-positron emission tomography. Chest 2006;129(2):393–401. [PubMed: 16478857]
43. Buck AK, Halter G, Schirrmeister H, et al. Imaging proliferation in lung tumors with PET: 18F-FLT versus 18F-FDG. J Nucl Med 2003;44(9):1426–1431. [PubMed: 12960187]
44. Chen W, Cloughesy T, Kamdar N, et al. Imaging proliferation in brain tumors with 18F-FLT PET: comparison with 18F-FDG. J Nucl Med 2005;46(6):945–952. [PubMed: 15937304]
45. Muzi M, Vesselle H, Grierson JR, et al. Kinetic analysis of 3'-deoxy-3'-fluorothymidine PET studies: validation studies in patients with lung cancer. J Nucl Med 2005;46(2):274–282. [PubMed: 15695787]
46. Vesselle H, Grierson J, Muzi M, et al. In vivo validation of 3'deoxy-3'-[(18)F]fluorothymidine ([(18)F]FLT) as a proliferation imaging tracer in humans: correlation of [(18)F]FLT uptake by positron emission tomography with Ki-67 immunohistochemistry and flow cytometry in human lung tumors. Clin Cancer Res 2002;8(11):3315–3323. [PubMed: 12429617]
47. Yamamoto Y, Nishiyama Y, Ishikawa S, et al. Correlation of 18F-FLT and 18F-FDG uptake on PET with Ki-67 immunohistochemistry in non-small cell lung cancer. Eur J Nucl Med Mol Imaging 2007;34(10):1610–1616. [PubMed: 17530250]
48. Yue J, Chen L, Cabrera AR, et al. Measuring tumor cell proliferation with 18F-FLT PET during radiotherapy of esophageal squamous cell carcinoma: a pilot clinical study. J Nucl Med 2010;51(4):528–534. [PubMed: 20237030]
49. van Westreenen HL, Cobben DC, Jager PL, et al. Comparison of 18F-FLT PET and 18F-FDG PET in esophageal cancer. J Nucl Med 2005;46(3):400–404. [PubMed: 15750150]
50. Ikeda G, Isaji S, Chandra B, Watanabe M, Kawarada Y. Prognostic significance of biologic factors in squamous cell carcinoma of the esophagus. Cancer 1999;86(8):1396–1405. [PubMed: 10526265]
51. Barwick T, Bencherif B, Mountz JM, Avril N. Molecular PET and PET/CT imaging of tumour cell proliferation using F-18 fluoro-L-thymidine: a comprehensive evaluation. Nucl Med Commun 2009;30(12):908–917. [PubMed: 19794320]
52. Oyama N, Ponde DE, Dence C, Kim J, Tai YC, Welch MJ. Monitoring of therapy in androgen-dependent prostate tumor model by measuring tumor proliferation. J Nucl Med 2004;45(3):519–525. [PubMed: 15001697]
53. Troost EG, Bussink J, Hoffmann AL, Boerman OC, Oyen WJ, Kaanders JH. 18F-FLT PET/CT for early response monitoring and dose escalation in oropharyngeal tumors. J Nucl Med 2010;51(6):866–874. [PubMed: 20484426]

54. Begg AC, Haustermans K, Hart AA, et al. The value of pretreatment cell kinetic parameters as predictors for radiotherapy outcome in head and neck cancer: a multicenter analysis. Radiother Oncol 1999;50(1):13–23. [PubMed: 10225552]
55. Wilson GD, Saunders MI, Dische S, et al. Pre-treatment proliferation and the outcome of conventional and accelerated radiotherapy. Eur J Cancer 2006;42(3):363–371. [PubMed: 16386890]
56. Bentzen SM, Atasoy BM, Daley FM, et al. Epidermal growth factor receptor expression in pretreatment biopsies from head and neck squamous cell carcinoma as a predictive factor for a benefit from accelerated radiation therapy in a randomized controlled trial. J Clin Oncol 2005;23(24):5560–5567. [PubMed: 16110017]
57. Eriksen JG, Steiniche T, Askaa J, Alsner J, Overgaard J. The prognostic value of epidermal growth factor receptor is related to tumor differentiation and the overall treatment time of radiotherapy in squamous cell carcinomas of the head and neck. Int J Radiat Oncol Biol Phys 2004;58(2):561–566. [PubMed: 14751528]
58. Eriksen JG, Steiniche T, Overgaard J. The influence of epidermal growth factor receptor and tumor differentiation on the response to accelerated radiotherapy of squamous cell carcinoma of the head and neck in the randomized DAHANCA 6 and 7 study. Radiother Oncol 2005;74:93–100. [PubMed: 15816106]
59. Bonner JA, Harari PM, Giralt J, et al. Radiotherapy plus cetuximab for squamous-cell carcinoma of the head and neck. N Engl J Med 2006;354(6):567–578. [PubMed: 16467544]
60. Yang YJ, Ryu JS, Kim SY, et al. Use of 3'-deoxy-3'-[18F]fluorothymidine PET to monitor early responses to radiation therapy in murine SCCVII tumors. Eur J Nucl Med Mol Imaging 2006;33(4):412–419. [PubMed: 16404598]
61. Apisarnthanarax S, Alauddin MM, Mourtada F, et al. Early detection of chemoradioresponse in esophageal carcinoma by 3'-deoxy-3'-3H-fluorothymidine using preclinical tumor models. Clin Cancer Res 2006;12(15):4590–4597. [PubMed: 16899606]
62. Mishani E, Abourbeh G, Eiblmaier M, Anderson CJ. Imaging of EGFR and EGFR tyrosine kinase overexpression in tumors by nuclear medicine modalities. Curr Pharm Des 2008;14(28):2983–2998. [PubMed: 18991714]
63. Lee FT, O'Keefe GJ, Gan HK, et al. Immuno-PET quantitation of de2–7 epidermal growth factor receptor expression in glioma using 124I-IMP-R4-labeled antibody ch806. J Nucl Med 2010;51(6):967–972. [PubMed: 20484439]
64. Harris AL. Hypoxia--a key regulatory factor in tumour growth. Nat Rev Cancer 2002;2(1):38–47. [PubMed: 11902584]
65. Malinen E, Sovik A, Hristov D, Bruland OS, Olsen DR. Adapting radiotherapy to hypoxic tumours. Phys Med Biol 2006;51(19):4903–4921. [PubMed: 16985278]
66. Nordsmark M, Bentzen SM, Rudat V, et al. Prognostic value of tumor oxygenation in 397 head and neck tumors after primary radiation therapy. An international multi-center study. Radiother Oncol. 2005
67. Koukourakis MI, Bentzen SM, Giatromanolaki A, et al. Endogenous Markers of Two Separate Hypoxia Response Pathways (hypoxia inducible factor 2 alpha and carbonic anhydrase 9) Are Associated With Radiotherapy Failure in Head and Neck Cancer Patients Recruited in the CHART Randomized Trial. J Clin Oncol. 2006
68. Tatum JL, Kelloff GJ, Gillies RJ, et al. Hypoxia: importance in tumor biology, noninvasive measurement by imaging, and value of its measurement in the management of cancer therapy. Int J Radiat Biol 2006;82(10):699–757. [PubMed: 17118889]
69. Movsas B, Chapman JD, Hanlon AL, et al. Hypoxic prostate/muscle pO2 ratio predicts for biochemical failure in patients with prostate cancer: preliminary findings. Urology 2002;60(4):634–639. [PubMed: 12385924]
70. Vergis R, Corbishley CM, Norman AR, et al. Intrinsic markers of tumour hypoxia and angiogenesis in localised prostate cancer and outcome of radical treatment: a retrospective analysis of two randomised radiotherapy trials and one surgical cohort study. Lancet Oncol 2008;9(4):342–351. [PubMed: 18343725]

71. Stewart GD, Gray K, Pennington CJ, et al. Analysis of hypoxia-associated gene expression in prostate cancer: lysyl oxidase and glucose transporter-1 expression correlate with Gleason score. Oncol Rep 2008;20(6):1561–1567. [PubMed: 19020742]
72. Carnell DM, Smith RE, Daley FM, Saunders MI, Bentzen SM, Hoskin PJ. An immunohistochemical assessment of hypoxia in prostate carcinoma using pimonidazole: implications for radioresistance. Int J Radiat Oncol Biol Phys 2006;65(1):91–99. [PubMed: 16563659]
73. Hockel M, Schlenger K, Aral B, Mitze M, Schaffer U, Vaupel P. Association between tumor hypoxia and malignant progression in advanced cancer of the uterine cervix. Cancer Res 1996;56(19):4509–4515. [PubMed: 8813149]
74. Fyles AW, Milosevic M, Wong R, et al. Oxygenation predicts radiation response and survival in patients with cervix cancer. Radiother Oncol 1998;48(2):149–156. [PubMed: 9783886]
75. Mees G, Dierckx R, Vangestel C, Van de WC. Molecular imaging of hypoxia with radiolabelled agents. Eur J Nucl Med Mol Imaging 2009;36(10):1674–1686. [PubMed: 19565239]
76. Tatum JL, Kelloff GJ, Gillies RJ, et al. Hypoxia: importance in tumor biology, noninvasive measurement by imaging, and value of its measurement in the management of cancer therapy. Int J Radiat Biol 2006;82(10):699–757. [PubMed: 17118889]
77. Mahy P, De BM, de GT, et al. Comparative pharmacokinetics, biodistribution, metabolism and hypoxia-dependent uptake of [18F]-EF3 and [18F]-MISO in rodent tumor models. Radiother Oncol 2008;89(3):353–360. [PubMed: 18649964]
78. Dehdashti F, Grigsby PW, Lewis JS, Laforest R, Siegel BA, Welch MJ. Assessing tumor hypoxia in cervical cancer by PET with 60Cu-labeled diacetyl-bis(N4-methylthiosemicarbazone). J Nucl Med 2008;49(2):201–205. [PubMed: 18199612]
79. Dence CS, Ponde DE, Welch MJ, Lewis JS. Autoradiographic and small-animal PET comparisons between (18)F-FMISO, (18)F-FDG, (18)F-FLT and the hypoxic selective (64)Cu-ATSM in a rodent model of cancer. Nucl Med Biol 2008;35(6):713–720. [PubMed: 18678357]
80. Busk M, Horsman MR, Jakobsen S, Bussink J, van der KA, Overgaard J. Cellular uptake of PET tracers of glucose metabolism and hypoxia and their linkage. Eur J Nucl Med Mol Imaging 2008;35(12):2294–2303. [PubMed: 18682937]
81. Christian N, Deheneffe S, Bol A, et al. Is (18)F-FDG a surrogate tracer to measure tumor hypoxia? Comparison with the hypoxic tracer (14)C-EF3 in animal tumor models. Radiother Oncol. 2010 %19.
82. Koh WJ, Rasey JS, Evans ML, et al. Imaging of hypoxia in human tumors with [F-18]fluoromisonidazole. Int J Radiat Oncol Biol Phys 1992;22(1):199–212. [PubMed: 1727119]
83. Rasey JS, Koh WJ, Evans ML, et al. Quantifying regional hypoxia in human tumors with positron emission tomography of [18F]fluoromisonidazole: a pretherapy study of 37 patients. Int J Radiat Oncol Biol Phys 1996;36(2):417–428. [PubMed: 8892467]
84. Nehmeh SA, Lee NY, Schroder H, et al. Reproducibility of intratumor distribution of (18)F-fluoromisonidazole in head and neck cancer. Int J Radiat Oncol Biol Phys 2008;70(1):235–242. [PubMed: 18086391]
85. Lee NY, Mechalakos JG, Nehmeh S, et al. Fluorine-18-labeled fluoromisonidazole positron emission and computed tomography-guided intensity-modulated radiotherapy for head and neck cancer: a feasibility study. Int J Radiat Oncol Biol Phys 2008;70(1):2–13. [PubMed: 17869020]
86. Lee N, Nehmeh S, Schoder H, et al. Prospective trial incorporating pre-/mid-treatment [18F]-misonidazole positron emission tomography for head-and-neck cancer patients undergoing concurrent chemoradiotherapy. Int J Radiat Oncol Biol Phys 2009;75(1):101–108. [PubMed: 19203843]
87. Feng M, Kong FM, Gross M, Fernando S, Hayman JA, Ten Haken RK. Using fluorodeoxyglucose positron emission tomography to assess tumor volume during radiotherapy for non-small-cell lung cancer and its potential impact on adaptive dose escalation and normal tissue sparing. Int J Radiat Oncol Biol Phys 2009;73(4):1228–1234. [PubMed: 19251094]
88. Gillham C, Zips D, Ponisch F, et al. Additional PET/CT in week 5–6 of radiotherapy for patients with stage III non-small cell lung cancer as a means of dose escalation planning? Radiother Oncol 2008;88(3):335–341. [PubMed: 18514339]

89. Das SK, Miften MM, Zhou S, et al. Feasibility of optimizing the dose distribution in lung tumors using fluorine-18-fluorodeoxyglucose positron emission tomography and single photon emission computed tomography guided dose prescriptions. Med Phys 2004;31(6):1452–1461. [PubMed: 15259648]

90. Flynn R, Barbee D, Bowen S, et al. Dose painting with intensity modulated proton therapy and intensity modulated x-ray therapy: A comparison. Med Phys 2007;34(6):2522–2523.

91. Alber M, Paulsen F, Eschmann SM, Machulla HJ. On biologically conformal boost dose optimization. Phys Med Biol 2003;48(2):N31–N35. [PubMed: 12587912]

92. Bowen S, Flynn R, Bentzen SM, Jeraj R. Effect of a biologically-based prescription function in IMRT dose optimization. Med Phys 2007;34(6):2524.

93. Thorwarth D, Eschmann SM, Paulsen F, Alber M. Hypoxia dose painting by numbers: a planning study. Int J Radiat Oncol Biol Phys 2007;68(1):291–300. [PubMed: 17448882]

94. Rickhey M, Bogner L. Application of the inverse Monte Carlo treatment planning system IKO for an inhomogeneous dose prescription in the sense of dose painting. Z Med Phys 2006;16(4):307–312. [PubMed: 17216756]

95. Sovik A, Malinen E, Skogmo HK, Bentzen SM, Bruland OS, Olsen DR. Radiotherapy adapted to spatial and temporal variability in tumor hypoxia. Int J Radiat Oncol Biol Phys 2007;68(5):1496–1504. [PubMed: 17674980]

96. Yang Y, Xing L. Towards biologically conformal radiation therapy (BCRT): selective IMRT dose escalation under the guidance of spatial biology distribution. Med Phys 2005;32(6):1473–1484. [PubMed: 16013703]

97. Muzik J, Soukup M, Alber M. Comparison of fixed-beam IMRT, helical tomotherapy, and IMPT for selected cases. Med Phys 2008;35(4):1580–1592. [PubMed: 18491552]

98. Korreman SS, Ulrich S, Bowen S, Deveau M, Bentzen SM, Jeraj R. Feasibility of dose painting using a volumetric modulated arc optimization technique. Acta Oncol. 2010 In press.

99. Kissick MW, Mo X, McCall KC, Schubert LK, Westerly DC, Mackie TR. A phantom model demonstration of tomotherapy dose painting delivery, including managed respiratory motion without motion management. Phys Med Biol 2010;55(10):2983–2995. [PubMed: 20436233]

100. Jingu K, Ariga H, Kaneta T, et al. Focal dose escalation using FDG-PET-guided intensity-modulated radiation therapy boost for postoperative local recurrent rectal cancer: a planning study with comparison of DVH and NTCP. BMC Cancer 2010;10:127. 127. [PubMed: 20374623]

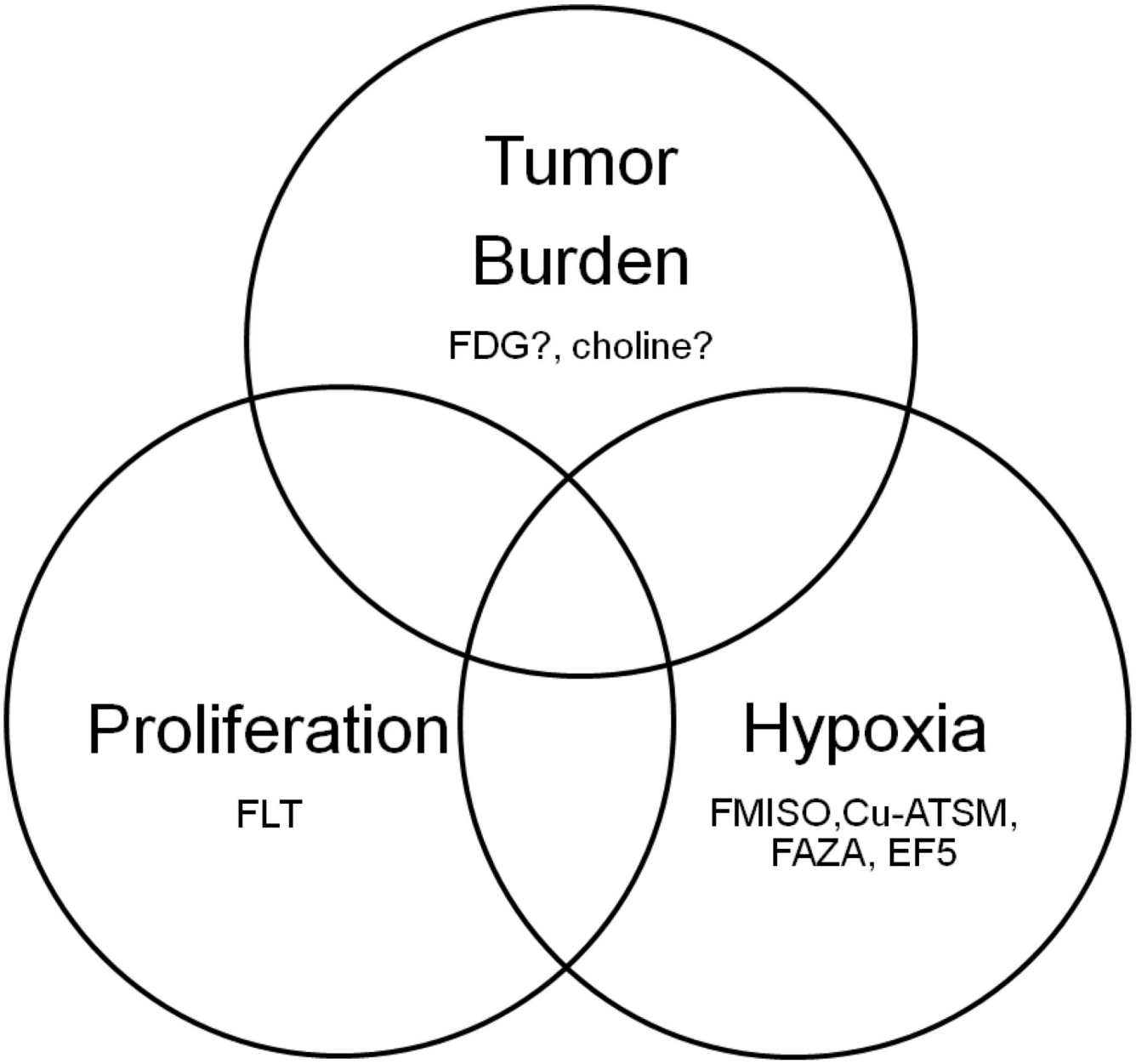

Figure 1.
Established clinical causes of local treatment failure after fractionated radiation therapy and selected PET tracers of interest as surrogates for these phenotypes.

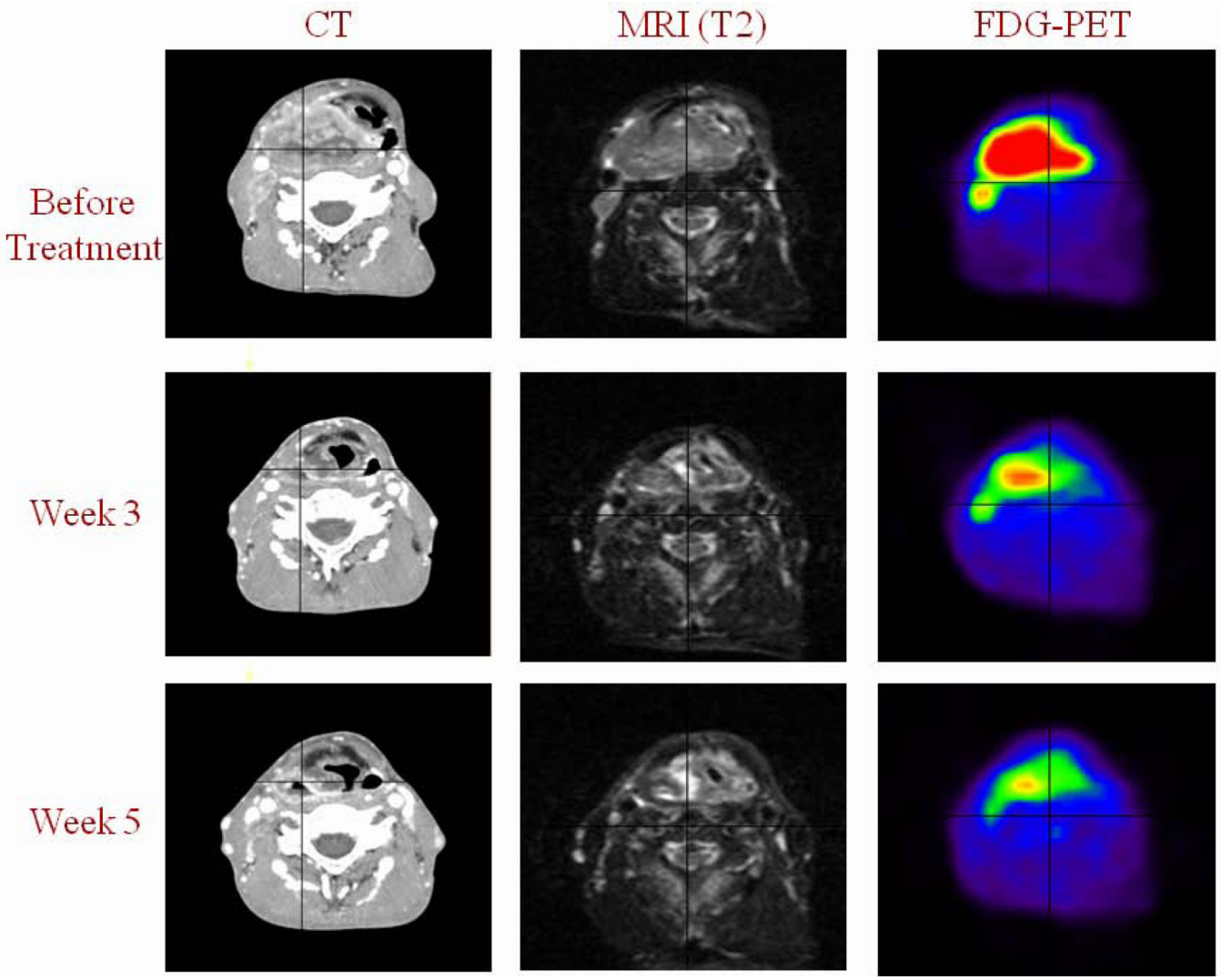

Figure 2.
Patient with a right-sided T4-N1-M0 hypopharyngeal squamous cell carcinoma receiving concomitant chemo-radiotherapy and imaged with intravenous contrast CT, MRI (T2 weighted sequence) and FDG PET before treatment and at the end of week 3 (30 Gy) and 5 (50 Gy). Primary tumor shrinkage is observed with all imaging modalities, but is more pronounced with FDG-PET.

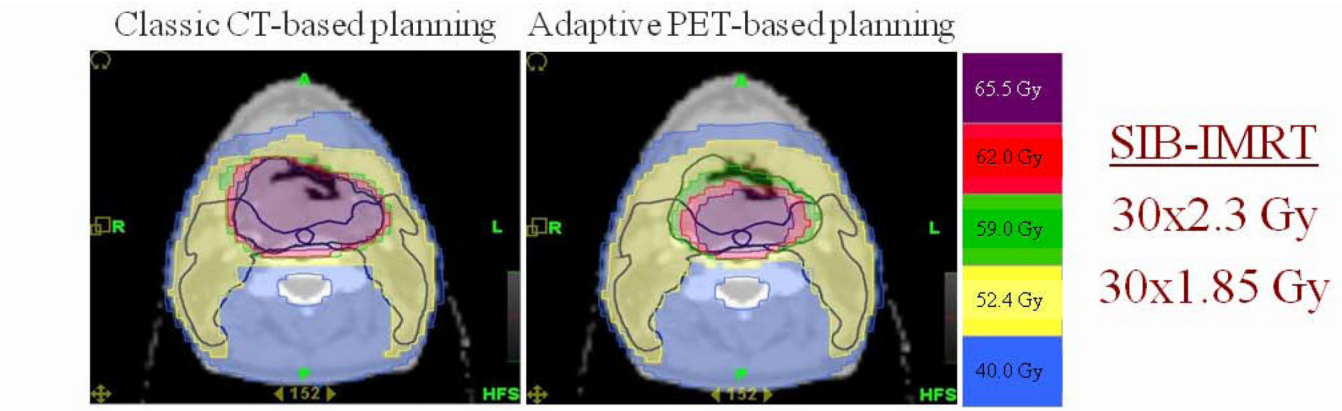

Planning	V_{10}	V_{50}	V_{80}	V_{90}	V_{95}	V_{100}
Classic CT-based	100%	100%	100%	100%	100%	100%
Adaptive CT-based	99%	100%	100%	85%	80%	66%
Classic PET-based	99%	99%	98%	83%	82%	81%
Adaptive PET-based	99%	100%	98%	73%	67%	58%

Figure 3.

Patient with a T3-N0-M0 posterior pharyngeal wall squamous cell carcinoma treated with simultaneous integrated boost IMRT. A total dose of 69 Gy (30 fractions of 2.3 Gy in 6 weeks) was prescribed to the primary tumor planning target volume (PTV), and 55.5 Gy (30 fractions of 1.85 Gy in 6 weeks) to the prophylactic nodal PTV. Intravenous-contrast CT and FDG-PET were performed before the start of radiotherapy and weekly during treatment. Target volumes and organs at risk were delineated on each CT study. On FDG PET scans, the GTVs were automatically segmented using a gradient-based algorithm. FDG-PET images were registered on the CT images with a rigid registration algorithm. Dose optimizations were performed at each time points on CT-based and PET-based images. Doses were then added to get the composite dose distribution. Compared with non-adaptive CT planning (classic CT-based), non-adaptive FDG-PET planning (classic PET-based) allows a significant reduction of the high dose volumes (V_{90}–V_{100}). While an adaptive CT-based plan allowed for a greater reduction in V_{90}–V_{100} isodose volumes, the largest effect was observed with the adaptive PET-based plan. In all scenarios, the lower isodose volumes were not reduced due to the non-adapted prophylactic irradiation of the nodal PTV.

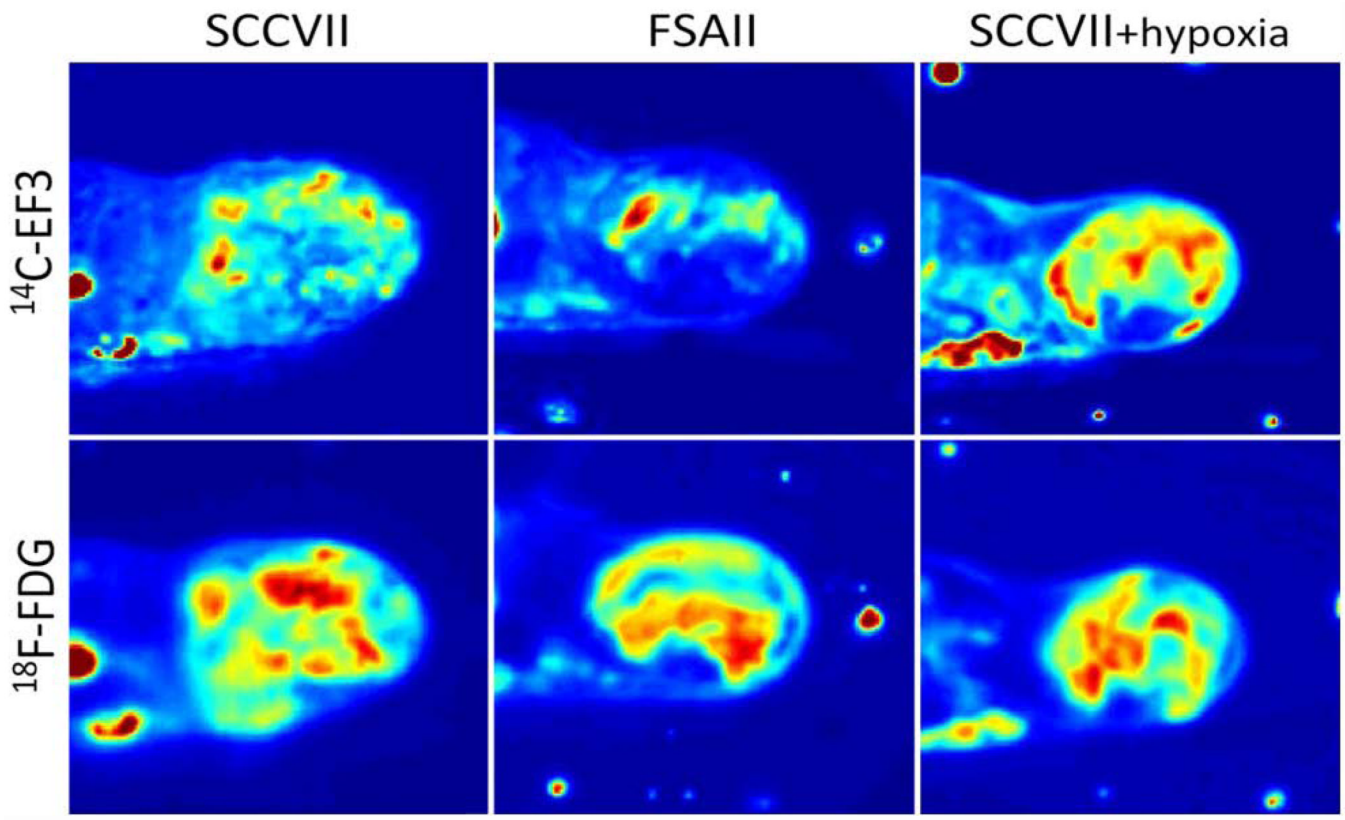

Figure 4.
Comparison between FDG and EF3 for the detection of hypoxia in C3Hf/Kam mouse FSA (fibrosarcoma) and SCCVII (squamous cell carcinoma) under air-breathing or 10% oxygen breathing. ^{14}C-EF3 (9.7 MBq) was injected in the tail vein followed 1h later by ^{18}F-FDG (17.6 MBq). One hour after the second injection, the mice were killed and processed for autoradiography. The ^{18}F-FDG images were obtained after a 45-min exposure. After a 48-h rest time allowing for ^{18}F decay, the sections were exposed for 56h to obtain the ^{14}C-EF3 distribution.

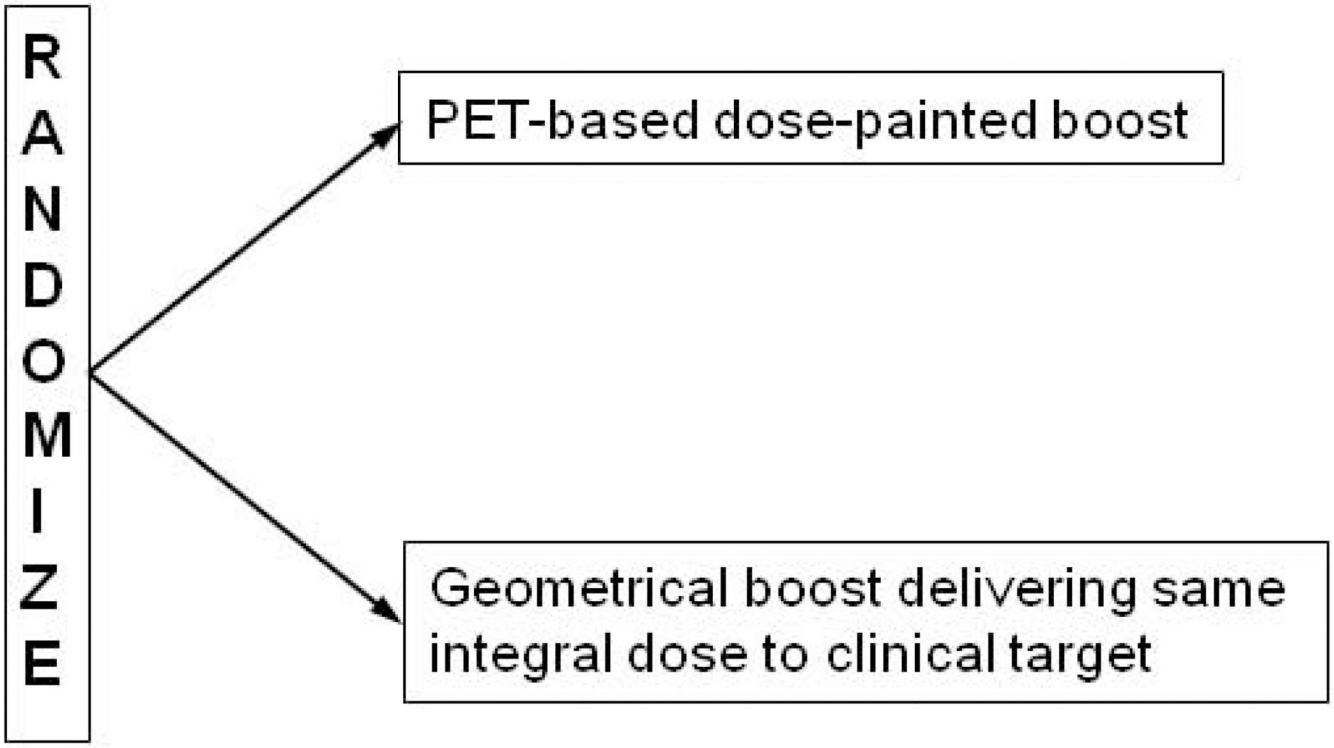

Figure 5.
Schematic representation of a proposed phase III trial of dose painting. See text for discussion.